Red Sea Outflow Experiment (REDSOX): Descent and initial spreading of Red Sea Water in the northwestern Indian Ocean

A.S. Bower (1), W.E. Johns (2), H. Peters (2) and D.M. Fratantoni(1)

(1) – Woods Hole Oceanographic Institution, Department of Physical Oceanography, Woods Hole, MA 02543 USA (E-mail: abower@whoi.edu; dfratantoni@whoi.edu)

(2) – Rosenstiel School of Marine and Atmospheric Science, University of Miami, 4600 Rickenbacker Causeway, Miami, FL 33149 USA (E-mail: wjohns@rsmas.miami.edu; hpeters@rsmas,.miami.edu)

Abstract

Two comprehensive surveys were carried out during 2001 to investigate the dense overflow and initial spreading of Red Sea Water (RSW) in the Gulf of Aden. The cruises were timed to coincide with the climatological maximum (February) and minimum (August) periods of outflow transport. The surveys included high-resolution CTD/lowered ADCP/ship-board ADCP observations in the descending plume and in the western gulf, and trajectories from 53 acoustically-tracked RAFOS floats released at the center of the equilibrated RSW (650 m). The measurements reveal a complicated descending plume structure in the western gulf with three main pathways for the high salinity RSW. Different mixing intensities along these pathways lead to variable penetration depths of the Red Sea plume between 450-900 m in the Gulf of Aden. The observations also revealed the hydrographic and velocity structure of large, energetic, deep-reaching mesoscale eddies in the gulf that fundamentally impact the spreading rates and pathways of RSW. Both cyclones and anticyclones were observed, with horizontal scales up to 250 km and azimuthal speeds as high as 0.5 m/s. The eddies appear to reach nearly to the sea floor and entrain RSW from the western gulf at mid-depth. Post-cruise analysis of SeaWiFs imagery suggests that some of these eddies form in the Indian Ocean and propagate into the gulf.

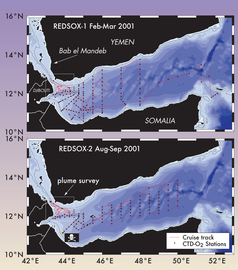

Figure 1: REDSOX-1 and REDSOX-2 Cruise Tracks
Ship tracks for Winter (REDSOX-1; upper panel) and Summer (REDSOX-2; lower panel) REDSOX cruises in the Gulf of Aden. Each cruise consisted of a high-resolution CTD/LADCP survey of the descending outflow plume and a broader-scale survey of the open gulf. The summer repetition of the winter cruise track was interrupted by a piracy attack 18 nm off the coast of Somalia, resulting in modification of the remaining survey. A total of 52 isobaric, acoustically-tracked RAFOS floats were also released during REDSOX at various locations in the gulf and tracked for one year.

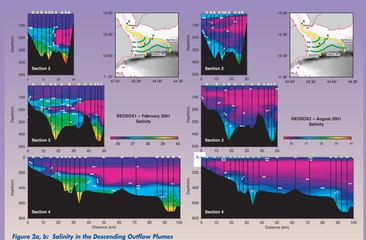

Figure 2a, b: Salinity in the Descending Outflow Plumes
Salinity sections across the Red Sea outflow plume at three locations progressing downslope from Bab el Mandeb, for Winter (left; maximum outflow) and Summer 2001 (right; minimum outflow). The locations of the sections are indicated in the map at upper right. All three sections show high-salinity Red Sea waters descending the slope that are focused into two deep channels, the "Northern Channel" and the "Southern Channel", which are indicated by the bold yellow lines on the maps. The bifurcation of the outflow into these two channels occurs just after Section 2. The Red Sea waters in the northern plume retain their high-salinity signal farther down the slope, suggesting less vigorous mixing and dilution along this path. Overlying the Red Sea waters in Winter (left) is a lens of fresh (and cool) Gulf of Aden thermocline water concentrated toward the northern side of the basin. On the southern side of the basin, a vein of shallow, mixed Red Sea waters can be seen intruding into the fresher Gulf waters; this vein has separated from the top of the outflow and reached equilibrium density within the ambient stratification. In Summer (right), both plumes are active but show lower salinities by up to 1.5 psu relative to the winter survey. This can be attributed mostly to enhanced mixing processes in the Bab el Mandeb strait during summer, where the combination of a weaker (and thinner) Red Sea outflow layer, and the intrusion of cold and fresh Gulf of Aden thermocline waters into the strait, lead to greater dilution of the Red Sea waters at the exit from the strait.

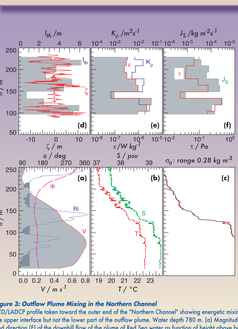

Figure 3: Outflow Plume Mixing in the Northern Channel
CTD/LADCP profile taken toward the outer end of the "Northern Channel" showing energetic mixing in the upper interface but not the lower part of the outflow plume. Water depth 780 m. (a) Magnitude (V) and direction (f) of the downhill flow of the plume of Red Sea water as function of height above bottom (h); Richardson number (Ri) showing regions of Ri<1/4. (b) Temperature (T) and salinity (S) showing signs of turbulent overturning in the salty and warm plume. (c) Thorpe-sorted (black) and observed (red) potential density (Thorpe, 1977). (d) Turbulent displacement from Thorpe-sorting (z) and RMS overturning scale, the Thorpe scale (lN), quantifying the turbulent overturning. Note that turbulent eddies partly span 20 m in depth. (e) Turbulent dissipation rate (e) and eddy diffusivity (Kr) estimated from lth and buoyancy frequency following Dillon [1982]. Note the large magnitude of Kr. (f) Interfacial turbulent stress (t) and turbulent salt flux (JS) estimated from lth.

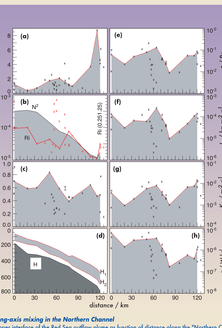

Figure 4: Along-axis mixing in the Northern Channel
Mixing in the upper interface of the Red Sea outflow plume as function of distance along the "Northern Channel," one realization (shaded and solid lines) and all data (+symbols). The depth extent (H1-H2) of the interface is shown in (d). Quantities are depth-averaged in (H1,H2) except velocity. (a) Thorpe scale (Thorpe, 1977), RMS turbulent overturning scale. (b) Squared buoyancy frequency (N2) and Richardson number (Ri), showing a decrease in stratification and Ri along the plume path. (c) Plume velocity averaged from the bottom to H1. (e) Interfacial turbulent stress (t). (f) Vertical turbulent salt flux (JS). (g) Eddy diffusivity (Kr). (h) Turbulent dissipation rate (e). Estimates of e, Kr, t and JS follow Dillon [1982]. These observations indicate that mixing is vigorous at the top interface of the northern plume, but that the deeper core of the plume little affected and retains its properties along the channel.

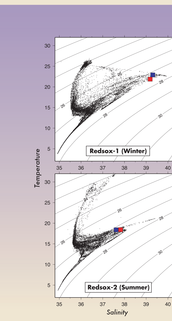

Figure 5: T-S Properties of Equilibrated Red Sea Water
Temperature-salinity scatterplots from all of the CTD stations collected in the Bab el Mandeb strait and western Gulf of Aden during the Winter (top) and Summer (bottom) cruises. The colored squares indicate the densest waters issuing into the Gulf of Aden from the northern and southern plumes during each season. The densest product waters are formed from the northern plume in winter, and the salinities of the product waters for both the northern and southern plumes are much higher (39.2-39.3 psu) than in summer (37.6-37.8 psu). However, the summer product waters are cooler by almost 4 C and are thus only slightly less dense than the winter product waters. The mixed remnants of the winter product waters can be seen as the salinity maximum just underlying the summer product waters.

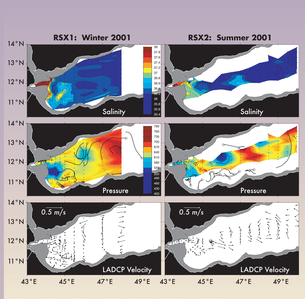

Figure 6: Hydrographic Properties, Float Tracks and Velocity at RSW level
Color shading indicates salinity (upper panels) and pressure (middle panels) on the 27.2 σ_Θ density surface, the main core density of Red Sea Water in the Gulf of Aden, during the Winter (left) and Summer (right) cruises. Superimposed on the pressure maps are preliminary 3-week track segments for RAFOS floats at RSW level (650 m; 'x' is at leading end of segment). Lower panels show LADCP velocity at the same level. The observations show that mesoscale eddies, both cyclonic and anticyclonic, are present in the gulf and strongly affect the spreading pathways and rates of RSW. During REDSOX-1, there were 2 large cyclones and 1 anticyclone observed, as well as some smaller features. During REDSOX-2, a well-defined large cyclone is evident between 47°- 49°E. More float tracks will become available as data processing is completed.

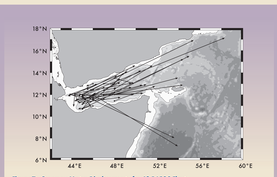

Figure 7: One-year Vector Displacements for 49 RAFOS Floats
Net vector displacements for all RAFOS floats launched in the gulf, ballasted for 650 m. The mean drift rate was 1.2-1.4 cm/s toward the ENE. Note that floats that escaped from the gulf did so toward the east; only two floats ended up south of Socotra Island.

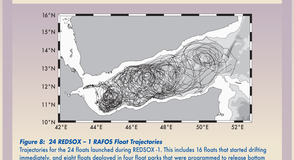

Figure 8: 24 REDSOX – 1 RAFOS Float Trajectories
Trajectories for the 24 floats launched during REDSOX-1. This includes 16 floats that started drifting immediately, and eight floats deployed in four float parks that were programmed to release bottom anchors at 2-month intervals and begin drifting. The tracks reveal the large loops associated with the Gulf of Aden eddies.

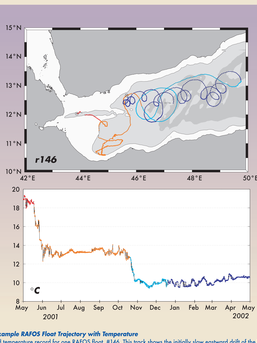

Figure 9: Example RAFOS Float Trajectory with Temperature
Trajectory and temperature record for one RAFOS float, #146. This track shows the initially slow eastward drift of the float as it left the Tajura Rift and meandered in the southwestern corner of the gulf. It then started looping cyclonically. It drifted much more rapidly eastward to the mouth of the gulf, then moved quickly back westward while executing repeated cyclonic loops. Sharp temperature decreases were observed when the float left the Tajura Rift and when it started looping cyclonically. Floats launched in the far western gulf typically drift slowly eastward until they encounter the large energetic eddies which can advect them quickly to the gulf entrance.

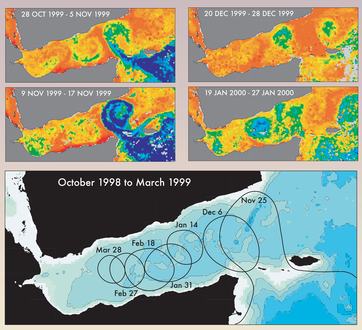

Figure 10: Generation of Translating Somali Current Rings
The top images show a time series of 9-day composite SeaWIFS surface chlorophyll images depicting the generation and translation of an anticyclonic ring in the eastern Gulf of Aden. The core of the ring is composed of relatively lifeless Somali Current water while the surrounding Gulf of Aden water is relatively productive. The lower panel shows a cartoon based on SeaWIFS frontal tracings illustrating ring generation. The retroflecting northward flow through the Socotra Passage collapses, pinching off an anticyclonic ring. The ring subsequently translates to the west at 5-8 cm/s.

References

Dillon, T. M., 1982. Vertical Overturns: A Comparison of Thorpe and Ozmidov Length Scales, J. Geophys. Res., 87, 9601-9613.

Thorpe, S. A., 1977. Turbulence and Mixing in a Scottish Loch, Philos. Trans. R. Soc. London A, 286, 125-181.

Acknowlegements

This project is being funded by the US National Science Foundation under grants OCE-98-18464 to the Woods Hole Oceanographic Institution and OCE-98-19506 to the Rosenstiel School of Marine and Atmospheric Science.